TiS Trends in Sciences
TRENDS IN SCIENCES 2027; 24(2): 13646
SPRINT Scholarly Publishing and Repository Integration Center
https://doi.org/10.48048/tis.2027.13646
RESEARCH ARTICLE

Nanocellulose-Enhanced Thin Film Nanocomposite Membrane Derived from Pineapple Leaf Waste for Methylene Blue Removal

Gubrina Rizka Maulida, Sri Aprilia*, Umi Fathanah, Fachrul Razi, Cut Meurah Rosnelly and Nasrul Arahman

Department of Chemical Engineering, Engineering Faculty, Universitas Syiah Kuala, Darusalam-Banda Aceh 23111, Indonesia

(*Corresponding author's e-mail: sriaprilia@usk.ac.id)

Received: 18 February 2026, Revised: 30 April 2026, Accepted: 10 May 2026, Published: 10 September 2026

Abstract

Thin-film nanocomposite (TFN) membranes incorporating nanocrystalline cellulose (NCC) derived from pineapple leaf waste were fabricated and evaluated for methylene blue removal from aqueous solutions. NCC was extracted through sequential alkaline treatment, bleaching, and sulfuric acid hydrolysis, yielding highly crystalline nanocellulose with an average particle size of 2.8 ± 0.5 nm and a crystallinity index of 87.23%. The TFN membranes were prepared via interfacial polymerization of piperazine and trimesoyl chloride on polyethersulfone ultrafiltration supports, with NCC loadings of 0, 0.1, 0.5, and 1.0 wt.% incorporated into the polyamide layer. Membrane characterization revealed that NCC incorporation markedly affected surface chemistry, morphology, and structural integrity. Fourier transform infrared spectroscopy confirmed the presence of cellulose-related functional groups, while scanning electron microscopy showed the formation of a dense and well-defined selective layer at moderate NCC concentrations. Thermal and mechanical analyses demonstrated enhanced thermal stability and tensile strength with increasing NCC content. Pure water permeability decreased with higher NCC loading, indicating increased membrane compactness, while dye rejection performance improved significantly. The TFN membrane containing 1.0 wt.% NCC exhibited the highest methylene blue rejection of 92.45%, whereas the membrane with 0.5 wt.% NCC provided an optimal balance between permeability and selectivity. These results highlight the effectiveness of pineapple leaf-derived NCC as a sustainable nanofiller for enhancing TFN membrane performance, offering a promising, low-cost approach for advanced wastewater treatment applications. In addition, the structure-performance relationship was further analyzed to elucidate the influence of NCC loading on membrane densification, permeability-selectivity trade-off, and dye rejection mechanisms. The limitations related to nanofiller dispersion and long-term stability are also discussed to provide a comprehensive evaluation of the developed membrane system.

Keywords: Thin-film nanocomposite membrane, Nanocrystalline cellulose, Pineapple leaf waste, Interfacial polymerization, Methylene blue removal, Wastewater treatment

Introduction

The textile industry plays a crucial role in global economic development; however, its rapid expansion has generated significant environmental challenges, particularly due to the discharge of synthetic dyes into aquatic ecosystems. Inefficient dye fixation during textile processing results in substantial dye losses, with an estimated 200,000 tons of dyes released annually into wastewater streams, posing serious ecological and public health concerns [1]. Among these dyes, methylene blue is a widely used cationic thiazine dye applied in coloring cotton, wood, and silk fibers owing to its high tinting strength and low cost [2]. Despite its industrial utility, methylene blue exhibits high water solubility and chemical stability, making it resistant to conventional wastewater treatment processes.

Prolonged exposure to methylene blue has been associated with toxic effects, including mutagenicity, neurotoxicity, and potential carcinogenic risks [3,4]. Consequently, the development of effective and sustainable technologies for dye-laden wastewater treatment remains an urgent priority.

Membrane-based separation technologies have emerged as promising solutions for dye removal due to their high efficiency, operational simplicity, and minimal chemical consumption. Among these, thin-film composite (TFC) membranes fabricated via interfacial polymerization are extensively employed in nanofiltration applications because of their high selectivity and tunable transport properties [5]. In TFC membranes, a dense polyamide selective layer formed at the interface between aqueous and organic phases governs separation performance by controlling solute rejection and water permeability. However, conventional TFC membranes often suffer from limitations such as permeability–selectivity trade-offs, fouling susceptibility, and restricted structural adaptability.

To overcome these drawbacks, TFN membranes have been developed by incorporating nanomaterials into the polyamide layer of TFC membranes. The introduction of nanofillers aims to modify surface chemistry, enhance hydrophilicity, and tailor pore structure, thereby improving membrane performance [5]. Various inorganic and carbon-based nanomaterials have been explored; however, concerns related to cost, environmental impact, and long-term sustainability have driven increasing interest in bio-based nanomaterials as eco-friendly alternatives.

Pineapple leaf waste represents an abundant and low-cost biomass resource, particularly in tropical regions. Its utilization not only reduces agricultural waste but also provides an economically viable raw material for membrane fabrication. However, large-scale application requires further evaluation of chemical consumption, waste generation, and process scalability. Future studies should include techno-economic and environmental impact assessments to validate the sustainability of this approach. NCC, derived from renewable biomass resources, has attracted considerable attention as a sustainable nanofiller due to its high aspect ratio, abundant hydroxyl functional groups, excellent mechanical strength, and inherent hydrophilicity. These properties enable NCC to enhance interfacial compatibility, promote water transport, and reinforce polymer matrices when incorporated into membrane systems. Previous studies have demonstrated the potential of cellulose-based nanomaterials to improve membrane permeability, mechanical stability, and dye rejection performance [6-8]. Nevertheless, most reported TFN membranes rely on nanocellulose sourced from wood, cotton, or agricultural residues such as jute and banana fibers, while alternative biomass sources remain underexplored.

Pineapple leaf waste represents an abundant and underutilized agricultural byproduct, particularly in tropical regions, and contains a high cellulose content suitable for nanocellulose extraction. To date, the application of pineapple leaf-derived nanocrystalline cellulose as a nanofiller in TFN membrane fabrication has not been systematically reported. Leveraging this waste resource offers a dual benefit: mitigating agricultural waste disposal issues while providing a low-cost and sustainable material for advanced membrane development.

In this study, nanocrystalline cellulose was extracted from pineapple leaf waste through alkaline treatment, bleaching, and sulfuric acid hydrolysis, and subsequently incorporated into the polyamide layer of TFN membranes via interfacial polymerization. The effects of NCC loading on membrane morphology, surface chemistry, permeability, mechanical strength, thermal stability, and methylene blue rejection were systematically investigated. This work aims to elucidate the structure–performance relationships of NCC-modified TFN membranes and demonstrate the feasibility of utilizing pineapple leaf waste as a sustainable nanofiller for high-performance wastewater treatment membranes.

Despite the increasing interest in nanocellulose-based TFN membranes, limited studies have systematically investigated the role of agricultural waste-derived NCC on the structure–performance relationship of polyamide layers. In particular, the effects of nanofiller dispersion, aggregation behavior, and loading-dependent performance remain insufficiently understood. Therefore, this study not only focuses on membrane fabrication but also aims to provide a deeper mechanistic understanding of how

NCC incorporation influences membrane morphology, transport properties, and separation performance.

Materials and methods

Materials

Pineapple leaf waste was collected from a local agricultural market in Indonesia and used as the raw material for nanocrystalline cellulose (NCC) extraction. Sodium hydroxide (NaOH), sodium hypochlorite (NaOCl, 5%), and sulfuric acid (H_2SO_4) were purchased from Sigma-Aldrich (Germany) and employed for chemical treatment during cellulose isolation. Polyethersulfone (PES, Ultrason® E 6020 P, Mw ≈ 72 kDa) supplied by BASF (Germany) was used as the base polymer for UF membrane fabrication. Polyvinylpyrrolidone (PVP, Mw ≈ 39 kDa) and dimethyl sulfoxide (DMSO), both obtained from Sigma-Aldrich (Germany), served as the pore-forming agent and solvent, respectively. For interfacial polymerization, piperazine (PIP, 99%) and trimesoyl chloride (TMC, 98%) were procured from Sigma-Aldrich (Germany), while n-hexane was used as the organic solvent. Distilled water was used throughout the study as a nonsolvent, washing medium, and feed solution.

Methods

Preparation of pineapple leaf powder

Fresh pineapple leaves were thoroughly washed with distilled water to remove surface contaminants and cut into segments approximately 5 cm in length. The cleaned leaves were sun-dried for 5 days and subsequently oven-dried at 105 °C for 12 h to remove residual moisture. The dried material was ground using a laboratory blender and sieved through a 200-mesh screen to obtain uniform pineapple leaf powder for subsequent nanocellulose extraction.

Extraction of cellulose

Ten g of pineapple leaf powder were treated with 200 mL of 15 wt.% NaOH solution at 80 °C for 90 min under continuous stirring to remove lignin and hemicellulose. The treated suspension was filtered, and the solid residue was washed repeatedly with distilled water until neutral pH was achieved. The delignified fibers were oven-dried and subsequently bleached by treating 1 g of the dried material with 20 mL of 5% NaOCl solution at 80 °C for 10 min. The bleached cellulose was filtered, thoroughly washed with distilled water, and oven-dried until an ivory-white appearance was obtained.

Preparation of NCC

Bleached cellulose (1 g) was subjected to acid hydrolysis using 10 mL of 2 M H_2SO_4 at 45 °C for 180 min under static conditions to selectively remove amorphous regions. The hydrolysis reaction was quenched by adding cold distilled water, followed by centrifugation at 8,000 rpm for 10 min to separate the hydrolyzed fraction. The precipitate was repeatedly washed with distilled water until neutral pH was attained.

The resulting suspension was aged at 20 °C for 24 h to enhance colloidal stability and then oven-dried to constant weight. The dried product was ground using a ceramic mortar to obtain nanocrystalline cellulose powder. The final NCC product exhibited particle dimensions in the nanometer range and was stored in a desiccator prior to use.

Fabrication of ultrafiltration membrane

Ultrafiltration membranes were fabricated using the phase inversion method. A casting solution was prepared by dissolving 15 wt.% PES and 1 wt.% PVP in 84 wt.% DMSO under continuous stirring at room temperature for 24 h until a homogeneous solution was obtained. The polymer solution was cast onto a clean glass plate using a casting knife with a nominal thickness of approximately 150 μm and a casting speed of ~15 cm s^{-1}.

Immediately after casting, the film was immersed in a coagulation bath containing distilled water at room temperature to induce phase separation. The membrane was allowed to detach spontaneously from the glass substrate, indicating complete solidification. The resulting UF membranes were stored in distilled water for at least 24 h to remove residual solvent and stabilize membrane structure. These membranes were designated as M1 (ultrafiltration support membrane).

Fabrication of TFC and TFN membranes

Thin-film composite and thin-film nanocomposite membranes were fabricated by interfacial polymerization on the surface of UF support membranes

(M1). The UF membranes were fixed on glass plates (10×10 cm^2) and covered with perforated acrylic sheets to ensure uniform contact. The dispersion of NCC in the organic phase was carefully controlled through continuous magnetic stirring to minimize aggregation prior to interfacial polymerization. Although no visible agglomeration was observed, it is acknowledged that nanoscale aggregation may still occur, which can influence membrane formation and performance.

An aqueous solution containing 2 wt.% piperazine (PIP) was prepared, while an organic solution consisting of 0.2 wt.% trimesoyl chloride (TMC) dissolved in n-hexane was used as the organic phase. For TFN membrane fabrication, NCC was dispersed into the TMC solution at concentrations of 0.1, 0.5, and 1.0 wt.% and magnetically stirred for 30 - 40 min until no visible agglomeration was observed.

The interfacial polymerization process was conducted by first pouring the PIP solution onto the UF membrane surface and allowing it to react for 5 min. Excess solution was removed using a rubber roller. Subsequently, the TMC or TMC–NCC solution was applied for 5 min to initiate polyamide layer formation at the interface. After draining the excess organic phase, the membranes were cured at 70 °C to enhance crosslinking and film stability. The fabricated membranes were designated as in Table 1. All membranes were stored in distilled water prior to characterization and performance testing.

Synthesis TFN nanofiltration membrane

Thin-film composite (TFC) and TFN membranes were fabricated by depositing polyamide layers onto the surface of preformed UF membranes using interfacial polymerization. The UF support membranes were placed onto glass substrates (10×10 cm^2), layered with perforated acrylic sheets to ensure uniform contact and mechanical stability. Two monomer solutions were prepared separately: an aqueous solution of 2 wt.% PIP and an organic solution of 0.15 wt.% trimesoyl chloride (TMC) in hexane. Both solutions were magnetically stirred for 24 h at ambient conditions to ensure complete dissolution and homogeneity. For TFN synthesis, NCC was added to the TMC solution at varying loadings (0, 0.1, 0.5, and 1 wt.%). The mixture was stirred until no visible aggregation remained, typically within 30 - 40 min.

Membrane coating was performed in 2 sequential steps. First, the PIP solution was gently poured over the membrane surface and allowed to react for 5 min, followed by removal of excess solution and leveling using a clean roller. Subsequently, the TMC-NCC solution was applied for 5 min to initiate interfacial polymerization at the membrane-aqueous interface. Excess organic solution was drained, and the membranes were cured on the mold at 70 °C to reinforce film integrity and enhance crosslinking. The synthesized membranes—denoted as M1 (UF-PES), M2 (TFC), and M3 - M5 (TFNs with NCC concentrations of 0.1%, 0.5%, and 1%, respectively)—were immersed in distilled water and stored for further characterization. The synthesis design of the TFC and TFN membranes can be seen in **Figure 1** and **Table 1**.

Table 1 TFN nanofiltration membrane synthesis.

UF Type Membrane	PIP concentration in H_2O (% wt)	TMC Concentration in n-Hexane (% w/v)	NCC (% wt)	Membrane Code
UF	-	-	-	M1
TFC	2	0.2	0	M2
TFN	2	0.2	0.1	M3
TFN	2	0.2	0.5	M4
TFN	2	0.2	1	M5

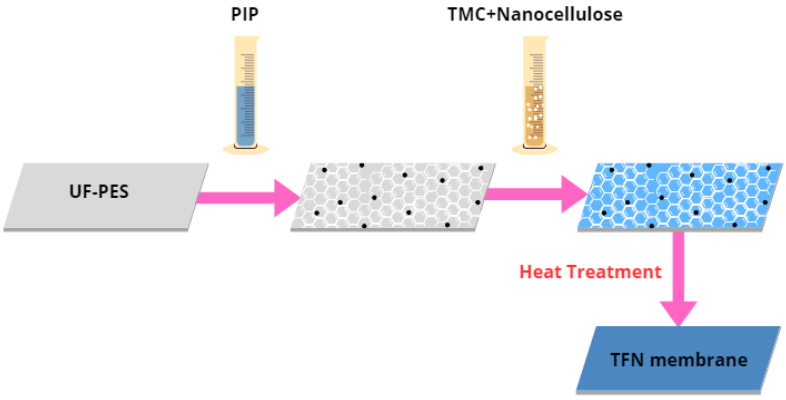


Figure 1 Schematic representation of the synthesis process for TFC and TFN membranes via interfacial polymerization.

Characterization

The characterization of nanocellulose involves a series of analytical techniques to evaluate its structural, morphological, and chemical properties. Morphological analysis is conducted using *Scanning Electron Microscopy* (SEM) to observe surface structure and particle distribution. The degree of crystallinity was determined by *X-Ray Diffraction* (XRD), which provides insights into the proportion of crystalline and amorphous phases. Functional group identification was performed using *Fourier Transform Infrared* (FTIR) spectroscopy to detect specific chemical bonds typical of cellulose. In addition, *Particle Size Analysis* (PSA) was employed to measure the size distribution of nanocellulose particles, ensuring they fall within the nanoscale range and are suitable for membrane applications.

The high crystallinity of NCC (87.23%) indicates effective removal of amorphous regions, which is expected to enhance mechanical reinforcement and interfacial compatibility within the polyamide matrix. This structural property plays a critical role in determining membrane performance, particularly in controlling polymer chain packing and transport pathways.

Membrane characterization was conducted to evaluate the physical and chemical performance of the synthesized membrane. The analysis included measurement of membrane permeability through pure water flux testing, which reflects the membrane's capacity to transport water under pressure. The chemical structure of the membrane was examined using FTIR spectroscopy to identify functional groups and confirm the presence of specific chemical bonds within the membrane matrix. The morphological structure of the membrane was observed using SEM, which provides information on surface topology, pore size, and pore distribution. Mechanical properties were assessed through tensile strength testing, which determines the membrane's resistance to mechanical stress and its structural integrity. Additionally, the thermal stability of the membrane was evaluated using thermal analysis techniques, which provide insights into the material's degradation behavior and operational temperature limits.

Methylene blue removal performance evaluation

The selectivity of the synthesized membranes toward methylene blue was evaluated to determine their efficiency in separating dye molecules from aqueous solutions. A feed solution of methylene blue with a concentration of 20 ppm was prepared using distilled water as the solvent. The filtration experiments were carried out under constant pressure in a dead-end membrane module system. During the test, the methylene blue solution was passed through the membrane, and the permeate was collected for analysis. The concentration of methylene blue in the permeate was quantified using a UV-Visible spectrophotometer, based on the absorbance at the maximum wavelength characteristic of methylene blue. The rejection efficiency of the membrane (R) was calculated using Eq. (1):

$$R = \frac{cf - cp}{cf} \times 100\% \quad (1)$$

where Cf is the concentration of MB in the feed solution (mg/L), and Cp is the concentration of MB in the permeate (mg/L).

Results and discussion

Characterization of the NCC

NCC yield analysis

NCC was isolated from pineapple leaf biomass via a 3-step protocol comprising delignification, bleaching, and acid hydrolysis. At each stage, the yield was determined by comparing post-treatment mass to the initial material input. During delignification, immersion in 15% NaOH at 80 °C for 90 min yielded 83.59%, reflecting effective lignin removal and substantial cellulose retention. Subsequent bleaching with sodium hypochlorite (NaOCl) further purified the delignified cellulose, resulting in a yield of 95.98%, indicative of efficient residual lignin elimination and improved fiber whiteness. The final acid hydrolysis step, conducted using 2 M sulfuric acid (H_2SO_4), reduced the yield to 52.02% due to the solubilization of amorphous domains and partial cellulose degradation. Nevertheless, this stage enhanced NCC crystallinity by selectively removing non-crystalline regions—a process whose efficiency is governed by acid concentration, thermal conditions, and hydrolysis duration [6].

NCC functional groups analysis

Figure 2 shows the presence of a hydroxyl group (–OH) at a wavenumber of 3,400 cm^{-1}, which indicates the hydrophilic nature of NCC due to the presence of hydrogen bonds between cellulose chains. Peaks at 610, 1,100, 1,370 and 2,800 cm^{-1} are associated with C-H stretching and bending vibrations, suggesting that the basic structure of the cellulose polymer is maintained after the isolation process. In addition, peaks at 1,630 - 1650 cm^{-1} are associated with C-O strain absorption that may have formed as a result of partial degradation of cellulose during acid hydrolysis and show evidence of water absorption. Overall, the FTIR spectrum confirms that the isolated NCC has a typical cellulose primary function group with a high level of purity [7].

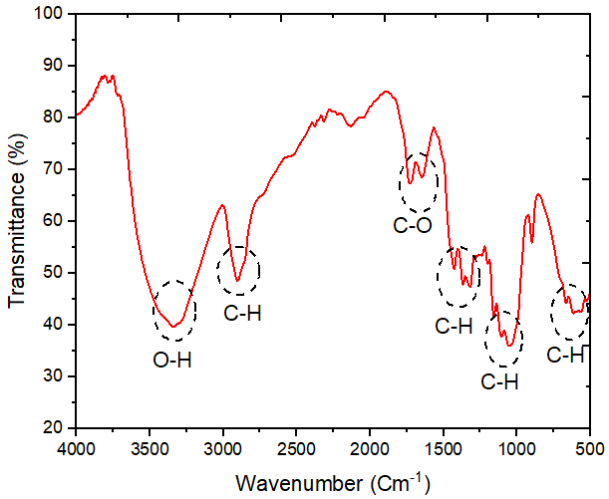


Figure 2 IR-Spectra of NCC extracted from pineapple leaves by acid hydrolysis.

The degree of NCC crystallinity analysis

The crystalline structure of NCC isolated from pineapple leaves was examined by XRD (**Figure 3**), revealing a sharp diffraction peak at $2\theta \approx 22.5°$, indexed to the (200) plane of cellulose I. This reflection confirms the dominance of highly ordered domains, consistent with plant-derived NCC exhibiting the Iα polymorph typical of parenchymal fibers. Minor signals near 16° and 34° correspond to residual amorphous regions, likely attributable to partially retained hemicellulose or insufficient hydrolysis of less-accessible cell wall fractions. Crystallinity Index (CrI) was calculated using the Segal method (Eq. (2)), yielding 87.23%, with 12.77% attributed to amorphous content.

$$CrI(\%) = \frac{I_{200} - I_{am}}{I_{200}} \times 100\% \quad (2)$$

where I_{200} is the maximum intensity of the (200) diffraction peak, and I_{am} is the minimum intensity at the amorphous baseline. This degree of crystallinity falls within the upper range reported for NCC from similar agricultural residues [8-10], supporting the efficiency of the extraction protocol. While the Segal method provides a convenient estimate, its reliance on peak height rather than integrated intensity may marginally overestimate CrI, especially in samples with overlapping profiles. Nonetheless, the predominance of crystalline domains is expected to enhance mechanical resilience, interfacial compatibility in membrane systems, and contribute to stable dispersion behavior in polymeric matrices of the final NCC product [8-10].

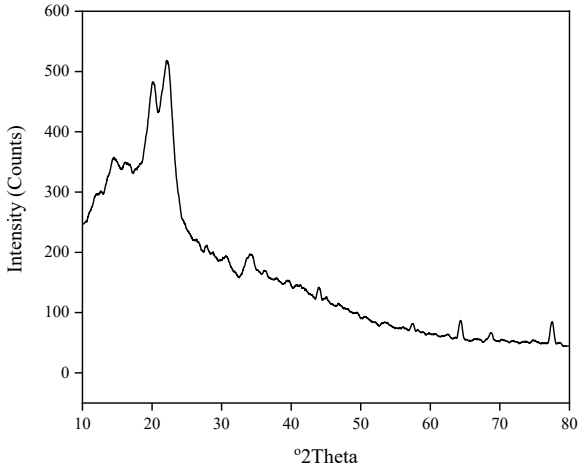


Figure 3 XRD analysis of NCC extracted from pineapple leaves by acid hydrolisis.

The NCC surface structure analysis

The SEM of the NCC surface structure shows in Figure 4. This figure illustrates the morphological features of NCC extracted from pineapple leaves, exhibiting rod-like, whisker-shaped structures at the nanoscale.

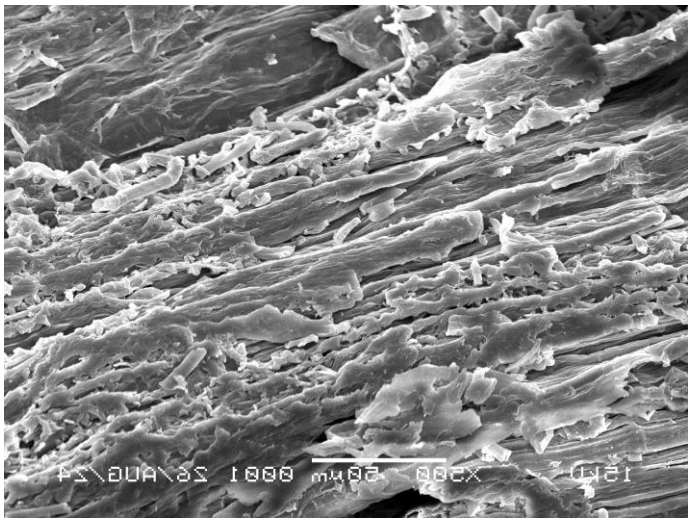


Figure 4 Structure surface of NCC extracted from peanapple leaves by acid hydrolysis.

The fibers are notably separated and reduced in size compared to native cellulose, reflecting the effective removal of lignin and hemicellulose through sequential delignification and bleaching treatments. The NCC particles demonstrate consistent nano-whisker geometry with a relatively uniform distribution, indicative of successful fragmentation of cellulose macrostructures into discrete nanoscale fibrils. The observed detachment and dispersion of the fibrils suggest minimal entanglement and strong structural

liberation from bulk cellulose. Dimensional reduction relative to untreated cellulose corroborates the chemical purification steps, as verified by yield analysis and X-ray diffraction (XRD) characterization.

Moreover, the SEM micrograph reveals a low degree of particle agglomeration, pointing to weak intermolecular interactions and favourable colloidal behaviour. This morphological trait is critical for enhancing NCC dispersion stability in liquid media, particularly within polymer or membrane matrices [11,12].

Particle size analysis

The NCC particle size analysis of pineapple leaves was performed using *a Particle Size Analyzer* (PSA) to determine the size distribution and homogeneity of the particles. The distribution of NCC particle size is shown in **Figure 5**.

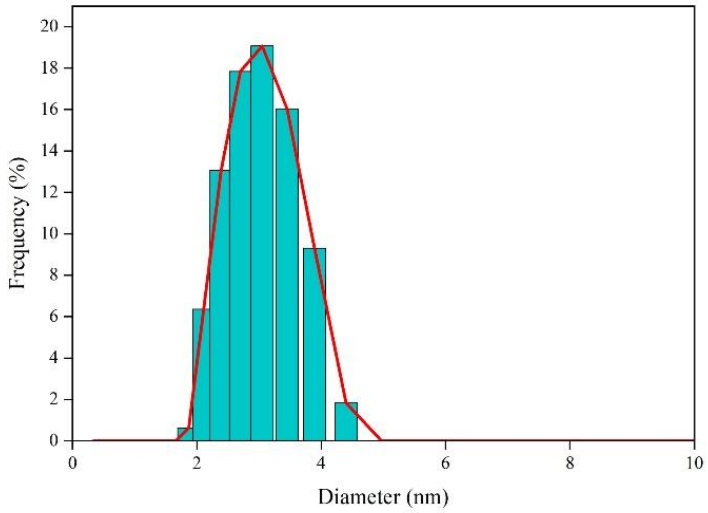


Figure 5 Particel size distribution of NCC extracted from peanapple leaves by acid hydrolysis.

The synthesized NCC shows a particle size distribution with a normal and asymmetric pattern, with most particles measuring < 100 nm. **Figure 5** shows that the average particle size is 2.8 ± 0.5 nm, which indicates the success of the acid isolation and hydrolysis process in producing nanometer-scale cellulose. This hydrolysis process leads to the degradation of the amorphous part of cellulose, resulting in fibers with smaller dimensions and high ratio aspects. **Figure 5** also shows the presence of particles of non-uniform size which indicates that there are still agglomerations or particles that are not fully dispersed in the medium. These results indicate that the dispersion or stabilization process of NCCs still needs to be optimized to obtain a more uniform size distribution [13].

The observed non-uniform particle size distribution also indicates partial aggregation of NCC, which may influence its dispersion behavior during interfacial polymerization. This aggregation can reduce the effective surface area and disrupt uniform incorporation within the polyamide layer. Although qualitative dispersion was achieved through stirring, quantitative evaluation such as zeta potential analysis is required to assess colloidal stability. Future studies will include zeta potential measurements to better understand dispersion stability and prevent agglomeration at higher NCC loadings.

Membrane characterization

Permeability coefficient of pure water

The membrane permeability coefficient test was performed using distilled water as a pure water sample, with pressure variations of 1, 2, and 3 bar for M1 membranes, as well as 3, 4, and 5 bars for M2, M3, M4, and M5 membranes. The measurement results are then presented in the form of a graph, with the change in pressure as the X axis and the flux value as the Y axis. The Lp values for each membrane are shown in **Figure 6** and **Table 2**.

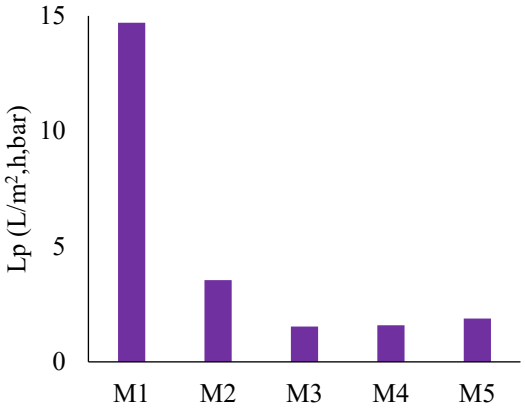


Figure 6 Coefficients permeability of pure water of 5 thin film nanocomposite membranes modified nanocellulose by ultrafiltration process.

Table 2 Purified Water Permeability (Lp) of thin film membranes.

No.	Membrane code	Lp (L/m²·h·bar)	Membrane type
1.	M1	14.70	UF
2.	M2	3.55	NF
3.	M3	1.53	NF
4.	M4	1.59	NF
5.	M5	1.88	NF

The pure water permeability (Lp) values of membranes M1 through M5 were determined to be 14.7, 3.55, 1.53, 1.59, and 1.88 L/m²·h·bar, respectively, as presented in Figure 6 and Table 2. Based on these values, membrane M1 is categorized as an (UF) membrane, consistent with the established UF Lp range of 10 - 50 L/m²·h·bar. In contrast, membranes M2 to M5 fall within the nanofiltration (NF) classification, corresponding to the NF range of 1.4 - 12 L/m²·h·bar [14]. This distinction affirms the inverse relationship between membrane pore size and water flux: NF membranes typically exhibit lower permeability due to denser polymer matrices and enhanced molecular sieving capability.

The observed decrease in water permeability with increasing NCC loading can be attributed to several structural factors. The incorporation of NCC into the polyamide layer promotes densification of the selective layer due to enhanced intermolecular interactions and hydrogen bonding. This results in reduced effective pore size and increased mass transfer resistance. Additionally, excessive NCC loading may lead to particle aggregation, which further blocks transport pathways. These effects collectively contribute to the classical permeability–selectivity trade-off observed in TFN membranes, where improved rejection is achieved at the expense of reduced water flux.

Figure 6 illustrates the influence of nanocrystalline cellulose (NCC) incorporation on Lp behaviour. A downward trend in permeability is observed with increasing NCC concentration, suggesting pore obstruction arising from NCC particle agglomeration. These aggregated domains may interfere with polymer chain packing and partially occlude transport pathways, leading to a diminished water flux. Notably, membranes with lower NCC loadings (e.g., M2) still show moderate Lp values, indicating that controlled NCC addition can enhance pore uniformity or facilitate water channelling when dispersion is optimal. This dual behaviour highlights the need for precise nanofiller dosing to balance membrane permeability and structural integrity.

The reduction in permeability with increasing NCC loading reflects the formation of a denser polyamide layer, driven by enhanced intermolecular interactions between NCC and the polymer matrix. This densification reduces effective pore size and increases mass transport resistance, resulting in lower water flux.

At the same time, the denser structure contributes to improved dye rejection, illustrating a typical permeability-selectivity trade-off.

Analysis of membrane function groups

FTIR spectroscopy is used to identify the surface chemical structure of the membraneM1, M2, M3, M4, and M5 as shown in **Figure 7**.

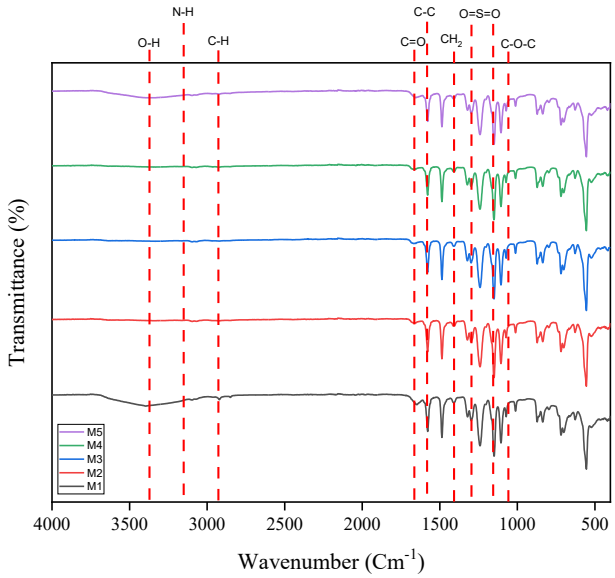


Figure 7 IR-spectra on thin film membranes modified nanocellulose extracted from peanapple leave by acied hydrolysis of M1, M2, M3, M4, and M5 membranes.

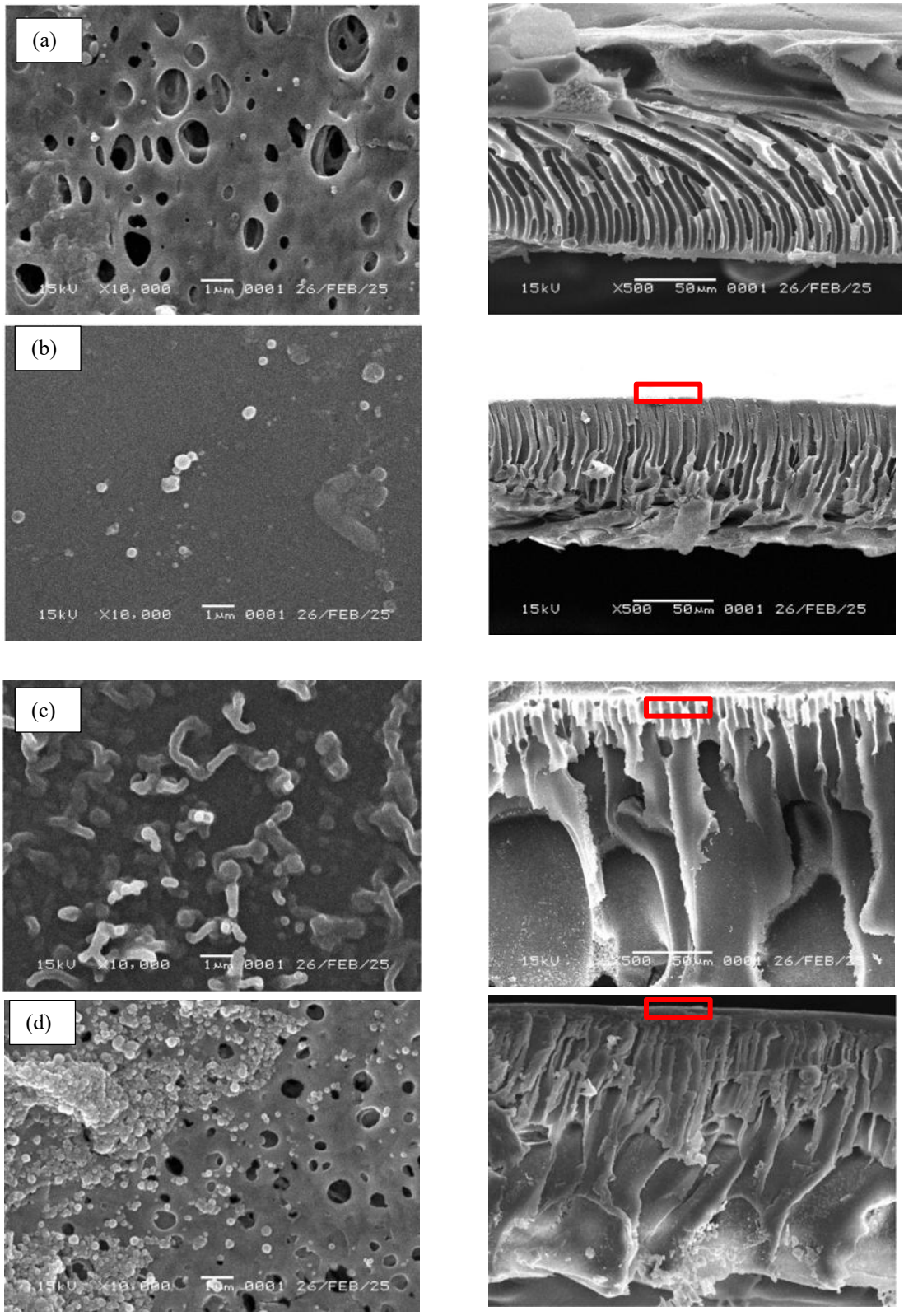
Figure 7 shows the FTIR spectrum of membranes M1, M2, M3, M4 and M5. This spectrum illustrates the differences in functional groups that occur due to the modification of materials with nanocellulose. The membrane of M1, which is based on polyethersulfone (PES), is characterized by an absorption band at 1,150 - 1,300 cm^{-1} indicating the presence of a sulfone group ($–SO_2^–$), as well as a peak at 1,600 - 1,700 cm^{-1} indicating an aromatic ring C=C. The M2 membrane has a typical polyamide spectrum with a primary absorption band at 1,620 - 1,660 cm^{-1} that represents the C=O strain vibration of the amide group, indicating that a polymerization process has occurred. In addition, bands at 1,500 - 1,570 cm^{-1} are associated with N–H and C–N vibrations, while bands at 3,200 - 3,400 cm^{-1} show N–H strain [15]

In the membranes M3, M4, and M5, which contain nanocellulose with concentrations of 0.1%, 0.5%, and 1%, respectively, there is an increase in band intensity at 3,300 - 3,500 cm^{-1} indicating the interaction of the O–H group of nanocellulose, as well as the appearance of a typical cellulose band at 1,030 - 1,100 cm^{-1} due to C–O–C vibration. The higher the concentration of nanocellulose, the intensity of the O–H band increases which suggests that the addition of nanocellulose additives can improve the hydrophilicity properties of the membrane [16,17].

The increase in –OH functional group intensity suggests enhanced membrane hydrophilicity due to NCC incorporation. However, this conclusion is currently based on indirect evidence. Contact angle measurements are recommended to quantitatively evaluate surface wettability and confirm the hydrophilic enhancement. Future work will include contact angle analysis to establish a direct correlation between surface chemistry and water transport behavior.

Membrane surface analysis

Figure 8 presents scanning electron microscopy (SEM) micrographs of the membrane surfaces and transverse cross-sections for samples M1 through M5.


(a)
15kV X10,000 1µm 0001 26/FEB/25
15kV X500 50µm 0001 26/FEB/25
(b)
15kV X10,000 1µm 0001 26/FEB/25
15kV X500 50µm 0001 26/FEB/25
(c)
15kV X10,000 1µm 0001 26/FEB/25
(d)
15kV X10,000 1µm 0001 26/FEB/25

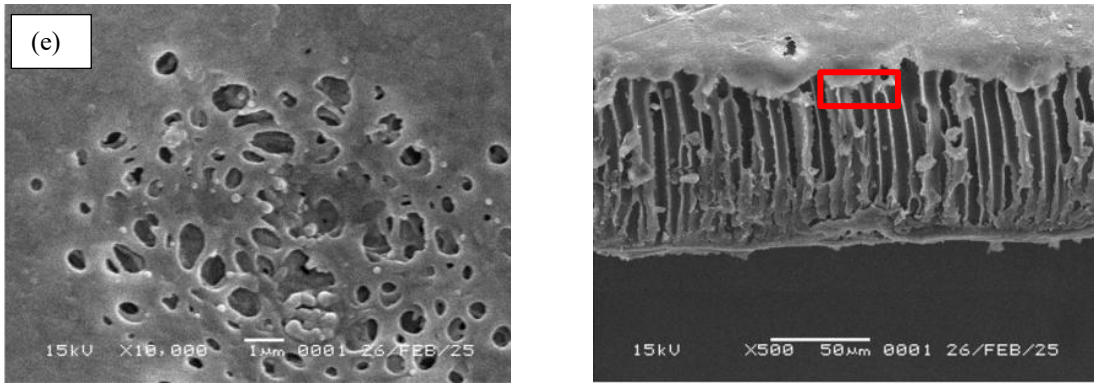


Figure 8 Structure surface and cross-section by SEM for thin film modified of nanocellulose composite membranes extracterd from pineaaple leave by acid hydrolysis, (a) M1, (b) M2, (c) M3, (d) M4 and (e) M5.

Surface observations reveal distinct structural features among the membrane variants. Membrane M1 displays a relatively open and homogenous pore network, characteristic of UF membranes with higher permeability. In contrast, membrane M2 exhibits a noticeably denser surface topology, indicative of a tighter polymer matrix and reduced pore size associated with NF behaviour.

For membranes M3, M4, and M5 engineered as TFN membranes with varying concentrations of NCC the top-surface SEM images show that NCC dispersion is relatively uniform at lower loadings. This uniformity supports enhanced structural regularity and selective transport channels. However, at elevated NCC concentrations, particle agglomeration becomes evident, leading to morphological disruption and non-uniform pore formation. Such clustering may hinder solvent accessibility and compromise membrane performance by introducing structural defects or hydraulic resistance.

Cross-sectional SEM images (×500 magnification) further delineate architectural transitions across membrane layers. Membrane M0 lacks a discernible active layer, confirming its absence of interfacial polymerization. Conversely, membranes M2 through M5 display a distinct thin selective layer atop the support structure, attributed to successful interfacial polymerization resulting in polyamide formation. The presence of this layer is central to achieving high selectivity in NF membranes and is consistent with controlled deposition of reactive monomers at the aqueous-organic interface [15,17].

Although SEM analysis confirms the whisker-like morphology and nanoscale structure of NCC, it is acknowledged that higher-resolution techniques such as Transmission Electron Microscopy (TEM) or Atomic Force Microscopy (AFM) would provide more precise visualization of particle size distribution and dispersion quality. Previous studies have demonstrated that TEM analysis typically reveals rod-like nanocrystals with high aspect ratios following sulfuric acid hydrolysis. Therefore, future work will incorporate TEM/AFM characterization to further validate the nanocrystalline structure of NCC.

Analysis of the thermal properties of the membrane

Thermogravimetric analysis was performed to evaluate the thermal stability as well as the decomposition pattern of the membrane-modification (M1 - M5). **Figure 9(a)** shows the TGA curves of the 5 membranes observed in the temperature range of 0 - 600 °C. In general, all samples show a gradual pattern of thermal degradation, which can be divided into several stages. The sharp decrease in mass in M3 and M5 indicates that the structure is more easily thermally degraded due to NCC. The M4 membrane showed a lower total mass decrease (64%), as well as a higher residue (36.0%). This shows that the modifications made by M4 contribute to better thermal stability due to the stronger crosslinking structure [18].

The DTA curve (**Figure 9(b)**) shows the thermal response of each membrane to heating. An early endothermic peak of about 100 - 150 °C was observed, which was associated with moisture release and volatility. Furthermore, in the temperature range of 230 - 270 °C, a mild endothermic peak appears that can be identified as the glass transition temperature (Tg) of the

membrane. These Tg values increase from 445 °C in M5 to 500 °C in M4, with the sequence M5 < M3 < M2 < M1 < M4 (**Table 3**). An increase in Tg indicates that the polymer's structure becomes more rigid and thermostable, consistent with the TGA result.

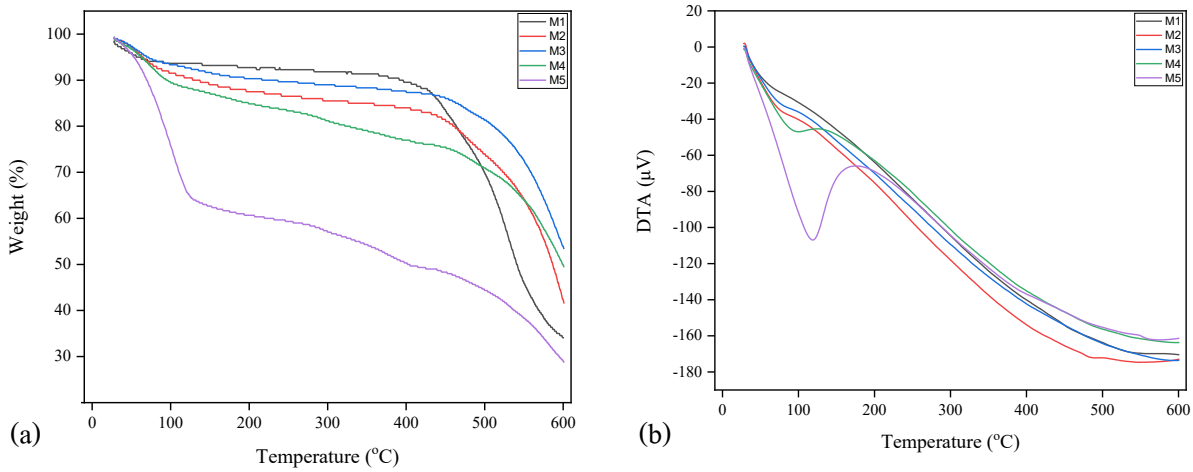


Figure 9 Thermal analysis by TGA (a) and DTA(b) curves on the thin film modified nanocellulose composite membranes M1, M2, M3, M4, and M5.

Table 3 TGA and DTA of membranes M1, M2, M3, M4, and M5.

Sample	Initial stage temperature (°C)	Decomposition stage (°C)	wt.% loss (Total)	Residual wt.%	Tg (°C)
M1	38 - 145	360 - 510	65.3	34.7	495
M2	40 - 148	355 - 500	69.3	30.7	475
M3	41 - 150	340 - 485	74.8	25.2	460
M4	39 - 144	365 - 515	64.0	36.0	500
M5	43 - 152	330 - 470	82.6	17.4	445

Analysis of the mechanical properties of the membrane

Membrane tensile strength tests are performed to evaluate the mechanical properties of the membrane, especially its resistance to applied tensile forces. A comparison of the tensile strength values of the membranes M1, M2, M3, M4 and M5 is shown in **Figure 10**.

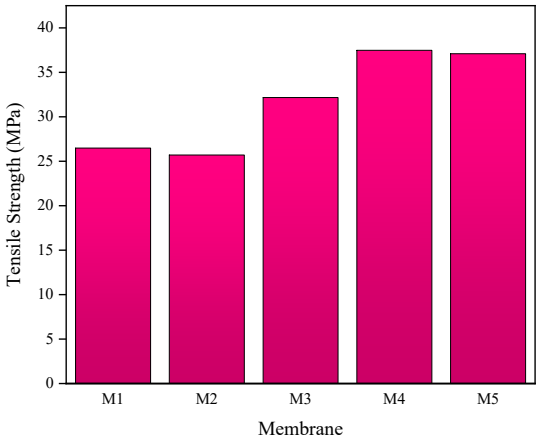


Figure 10 Tensile strength of thin film modified nanocellulose composite membrane.

Figure 10 shows that the membranes M1 and M2 have low tensile strengths, of 26.478 and 25.702 MPa, respectively, reflecting the limitations of the mechanical properties of the membrane without nanomaterial modification. On the M3 membrane (TFN with NCC 0.1%), the tensile strength value increases to 32.161 MPa. This increase correlates with the formation of hydrogen bonds between NCCs and polymer chains, which strengthen intermolecular interactions and affect membrane structure at the nanoscale. The membranes of M4 (TFN with NCC 0.5%), and M5 (TFN with NCC 1%), achieve the highest tensile strength, which is 37.472 and 37.086 MPa. Higher concentrations of NCC provide maximum reinforcement to the polymer matrix. However, the very small difference between M4 and M5 indicates that at these concentrations a saturation point has occurred, where the addition of additional NCC no longer significantly increases mechanical strength [19].

Membrane performance

Membrane rejection of methylene blue

Membrane rejection against *methylene blue* (MB) is an important parameter in assessing the effectiveness of the membrane in retaining dye molecules during the filtration process. The effect of different NCC concentrations on membranes on MB rejection is shown in **Figure 11**.

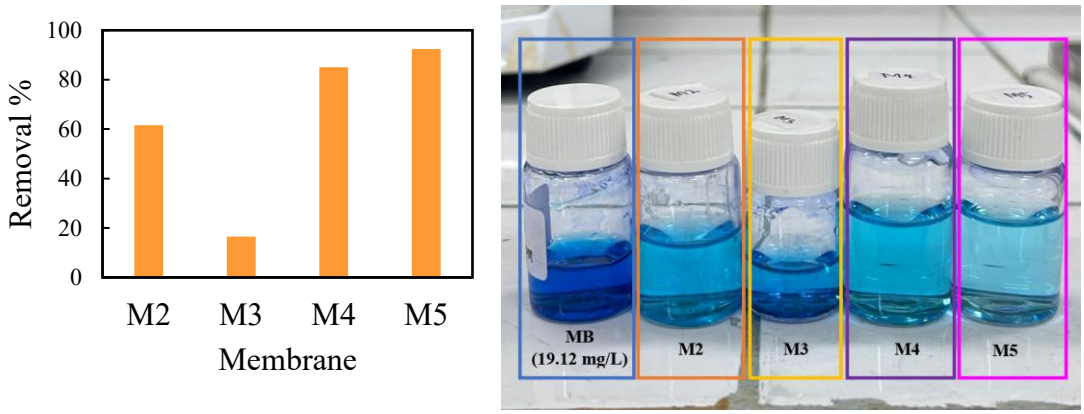


Figure 11 Percent of removal of the MBB with the thin film nanocellulose composite membrane.

Figure 11 illustrates the influence of membrane type and NCC content on the rejection performance of Methylene Blue. TFC membrane (M2) reduced MB concentration from 19.12 to 7.35 mg/L, achieving a rejection efficiency of 61.57%. By comparison, TFN membranes M3, M4, and M5 fabricated with incremental NCC loadings exhibited varying rejection outcomes: 16.5% (M3), 85.1% (M4), and 92.45% (M5). These results underscore the critical role of NCC incorporation in modulating membrane selectivity and functional performance.

The visible clarity of filtrates produced by M4 and M5, as depicted in **Figure 11**, corroborates their superior MB removal capacity relative to M2. This enhancement is attributed to the strategic introduction of NCC nanomaterials, which elevate membrane hydrophilicity and facilitate preferential water passage while impeding dye molecule transport. The improved separation is likely driven by intensified hydrogen bonding interactions and reinforced interfacial polymer integrity, yielding denser selective layers with tailored rejection capabilities.

However, membrane M3-prepared with 0.5 wt.% NCC-demonstrated markedly lower rejection efficiency. This decline is plausibly linked to nanoparticle agglomeration during interfacial polymerization, which can disrupt active layer homogeneity and generate structural defects. Such imperfections compromise dye-selective pathways, diminishing separation performance. These findings reinforce the necessity of optimizing NCC loading to balance dispersion quality, membrane architecture, and molecular sieving efficacy [16].

The enhanced rejection performance can be attributed to a combination of size exclusion and increased electrostatic interactions between the

membrane surface and dye molecules. The presence of NCC introduces additional hydroxyl groups, which enhance membrane hydrophilicity and contribute to improved separation efficiency.

The incorporation of NCC is also expected to improve antifouling properties due to increased surface hydrophilicity and reduced adsorption of organic foulants. Hydrophilic surfaces generally form a hydration layer that inhibits foulant attachment. However, antifouling performance was not experimentally evaluated in this study. Future investigations will include flux recovery ratio (FRR) analysis and fouling resistance tests using model foulants and real wastewater to validate practical applicability.

To further evaluate the performance of the developed membrane, a comparison with recent TFN and nanocellulose-based membranes reported in the literature has been conducted. The obtained rejection of 92.45% is comparable to or higher than many reported systems, indicating the competitiveness of pineapple leaf-derived NCC as a sustainable nanofiller. A detailed comparison table is provided to highlight the relative performance in terms of permeability and rejection.

To evaluate the competitiveness of the developed TFN membrane, a comparison with recently reported nanocellulose-based and TFN membranes was conducted, as summarized in **Table 4**. The results indicate that the membrane developed in this study achieves comparable or superior methylene blue rejection (92.45%) while utilizing a low-cost and sustainable nanofiller derived from pineapple leaf waste.

Table 4 Comparison of TFN and nanocellulose-based membranes for dye removal.

Membrane Type	Nanofiller	Dye	Permeability (L m^{-2} h^{-1} bar^{-1})	Rejection (%)	Key Findings	Ref
TFN membrane	CNC (wood-derived)	MB	2.1 - 3.5	85 - 91	Improved hydrophilicity and rejection due to hydrogen bonding	DOI: 10.1155/2022/5816063
TFN membrane	Cellulose nanocrystals	MB	1.8 - 2.7	88 - 93	Enhanced selectivity but slight permeability reduction	DOI: 10.1063/5.0080210
TFN membrane	Nanocellulose (jute/biomass)	Dye (cationic)	1.5 - 2.5	80 - 90	Improved mechanical strength and dye removal	DOI: 10.30564/jees.v7i1.7476
TFN membrane	CNC + polymer matrix	MB	1.2 - 2.0	85 - 92	Trade-off between permeability and selectivity observed	DOI: 10.1063/5.0119503
This work	NCC (pineapple leaf waste)	B	1.53 - 1.88	92.45	Sustainable biomass source; high rejection with good mechanical stability	This study

Compared to previously reported TFN membranes, the present membrane demonstrates competitive rejection performance while maintaining acceptable permeability. The improved performance is attributed to the incorporation of NCC, which enhances hydrophilicity and promotes the formation of a denser polyamide layer. Notably, the use of pineapple leaf waste as a precursor provides an additional advantage in terms of sustainability and resource utilization, which is rarely addressed in comparable studies.

Although the developed TFN membranes demonstrate promising separation performance, long-term operational stability has not been evaluated in this study. In particular, the potential leaching of NCC from the polyamide layer under continuous filtration conditions remains an important consideration. Future work will include extended filtration experiments and leaching analysis to assess membrane durability and structural integrity.

Conclusions

This study demonstrates the successful synthesis of TFN membranes incorporating with NCC extracted from pineapple leaf biomass via acid hydrolysis. The resulting NCC-characterized by high crystallinity (87.23%), nanoscale particle dimensions (2.8 ± 0.5 nm), and a well-defined whisker morphology proved to be a structurally compatible nanofiller for interfacial polymerization. Its integration into the polyamide layer led to significant enhancements in mechanical strength,

thermal stability, and surface hydrophilicity, as confirmed by FTIR, TGA/DTA, and SEM analyses. Performance testing revealed that the TFN membrane containing 1 wt.% NCC (M5) achieved the highest methylene blue rejection (92.45%), while the 0.5 wt.% NCC membrane (M4) provided the optimal trade-off between water permeability and dye selectivity. Importantly, the findings highlight a threshold in NCC loading: excessive concentrations promoted agglomeration, disrupting membrane homogeneity and diminishing flux performance. The work contributes a sustainable and functionally tuneable platform for membrane design, and future optimization should focus on controlling NCC dispersion, refining interfacial polymer morphology, and scaling the process for broader wastewater treatment applications. Although the developed membrane demonstrates promising performance, further investigations are required to evaluate long-term operational stability, antifouling properties, and large-scale applicability. These aspects are essential to validate the practical implementation of the proposed membrane system.

Acknowledgements

We would like to thank the funder of the Research and Community Service Institute of Syiah Kuala University, Ministry of Higher Education, Science and Technology in accordance with the Letter of Agreement and Assignment for the Implementation of Master's Thesis Research for the 2025 with the Number: 202/UN11.L1/PG.01.03/DPPM/2025.

Declaration of generative AI in scientific writing

The authors declare that generative artificial intelligence technology (ChatGPT) was used to a limited extent to assist with language editing and clarity of the manuscript. All scientific content, analysis, and conclusions are the sole responsibility of the authors.

CRediT author statement

Geubrina Rizqa Maulida: Data Curation; Methodology; Writing-Original draft preparation. **Sri Aprilia**: Conceptualization; Supervision; Project administration; Formal Analysis; Writing - Reviewing and Editing. **Umi Fathanah**: Supervision; validation. **Fachrul Razi**: Supervision; Writing - Reviewing and Editing. **Cut Meurah Rosnelly**: Validation; Formal Analysis; Validation. **Nasrul AR**: Validation; Data Curation; Writing - Reviewing and Editing.

References

[1] H Tsade Kara, ST Anshebo, FK Sabir and G Adam Workineh. Removal of methylene blue dye from wastewater using periodiated modified nanocellulose. *International Journal of Chemical Engineering* 2021; **2021(1)**, 9965452.

[2] N Benosmane, B Boutemeur, SM Hamdi and M Hamdi. Removal of methylene blue dye from aqueous solutions using polymer inclusion membrane technology. *Applied Water Science* 2022; **12(5)**, 104.

[3] OS Bayomie, H Kandeel, T Shoeib, H Yang, N Youssef and MM El-Sayed. Novel approach for effective removal of methylene blue dye from water using fava bean peel waste. *Scientific Reports* 2020; **10(1)**, 7824.

[4] JM Luque-Alled, L Martínez-Izquierdo, P Gorgojo, C Téllez and J Coronas. Organic solvent-free fabrication of thin film polyamide/zeolitic imidazolate framework membranes for removal of dyes from water. *Chemical Engineering Journal* 2023; **470**, 144233.

[5] WJ Lau, S Gray, T Matsuura, D Emadzadeh, JP Chen and AF Ismail. A review on polyamide thin film nanocomposite (TFN) membranes: History, applications, challenges and approaches. *Water Research* 2015; **80**, 306-324.

[6] F Whba, F Mohamed, MI Idris, & MS Yahya. (2022). Characterization of Cellulose Nanocrystals (CNCs) derived from Microcrystalline Cellulose (MCC) synthesized using acid hydrolysis method, Available at https://doi.org/10.21203/rs.3.rs-2078344/v2, accessed February 2026.

[7] MS Rana, MA Rahim, MP Mosharraf, MFK Tipu, JA Chowdhury, MR Haque, S Kabir, MS Amran and AA Chowdhury. Morphological, spectroscopic and thermal analysis of cellulose nanocrystals extracted from waste jute fiber by acid hydrolysis. *Polymers* 2023; **15(6)**, 1530.

[8] V Raju, R Revathiswaran, KS Subramanian, KT Parthiban, K Chandrakumar, EV Anoop and CJ Chirayil. Isolation and characterization of nanocellulose from selected hardwoods, viz.,

Eucalyptus tereticornis Sm. and *Casuarina equisetifolia* L., by steam explosion method. *Scientific Reports* 2023; **13(1)**, 1199.

[9] K Vasić, M Dokl, Ž Knez and M Leitgeb. Isolation and characterization of nanocellulose from *Polypodiophyta* fern using chemo-mechanical method. *Biomimetics* 2024; **9(10)**, 624.

[10] SM Beyan, TA Amibo, SV Prabhu and AG Ayalew. Production of nanocellulose crystal derived from enset fiber using acid hydrolysis coupled with ultrasonication, isolation, statistical modeling, optimization, and characterizations. *Journal of Nanomaterials* 2021; **2021**, 7492532.

[11] DM Fellicia, TY Rus and AM Sulaiman. Isolation and extraction of microcellulose from pineapple leaves fiber. *Mechanics Exploration and Material Innovation* 2024; **1(2)**, 61-66.

[12] MH Hemida, H Moustafa, S Mehanny, M Morsy, EN Abd El Rahman and MM Ibrahim. Valorization of Eichhornia crassipes for the production of cellulose nanocrystals further investigation of plethoric biobased resource. *Scientific Reports* 2024; **14(1)**, 12387.

[13] ESA Rashid, A Gul, WAH Yehya and NM Julkapli. Physico-chemical characteristics of nanocellulose at the variation of catalytic hydrolysis process. *Heliyon* 2021; **7(6)**, e07267.

[14] M Mulder. *Basic principles of membrane technology*. Springer, Dordrecht, Netherlands, 1996.

[15] M Hashemibeni, E Ameri, J Hashemibeni and H Seifi. Synthesis of nanocomposite membranes embedded with cellulose nanocrystals and their application to filtrate of arsenic aqueous solutions. *Desalination and Water Treatment* 2022; **247**, 17-27.

[16] D Liu, J Liu, S Lin, X Wei and MJ Guo. Preparation and characterization of cellulose nanocrystals with different aspect ratios as nano-composite membrane for cationic dye removal. *SN Applied Sciences* 2019; **1(12)**, 1596.

[17] EPN Ntone, S Abd Rahman, RA Samah, MSA Wahab, ZA Jawad and H Hasbullah. A comparison study on performance of thin film composite membrane embedded with graphene oxide for acetaminophen, diclofenac and ibuprofen separation from waste water. *Chemical Engineering Research and Design* 2023; **195**, 28-37.

[18] AI Syahrul, MD Rosyidin, S Hidayat, K Khaerunisa, N Soraya, NH Sari and S Syahrul. Characterization of nanocellulose from banana stem fiber and its bionanocomposite as a thermal insulation material. *Dinamika Teknik Mesin* 2025; **15(1)**, 65-75.

[19] H Wang, J Wu, B Huang and QL Lu. One-pot synthesis of UPy-functionalized nanocellulose under mechanochemical synergy for high-performance epoxy nanocomposites. *Polymers* 2022; **14(12)**, 2428.